

Photocytotoxicity of a New Rh<sub>2</sub>(II,II) Complex: Increase in Cytotoxicity upon Irradiation Similar to That of PDT Agent HematoporphyrinAlfredo M. Angeles-Boza,<sup>†</sup> Patricia M. Bradley,<sup>‡</sup> Patty K.-L. Fu,<sup>§</sup> Mikhail Shatruk,<sup>†</sup> Matthew G. Hilfiger,<sup>†</sup> Kim R. Dunbar,<sup>\*†</sup> and Claudia Turro<sup>\*‡</sup>

Department of Chemistry, The Ohio State University, Columbus, Ohio 43210,  
Department of Chemistry, Texas A&M University, College Station, Texas 77842, and  
Food and Drug Administration, College Park, Maryland 20740

Received January 17, 2005

A new type of heteroleptic dirhodium complex *cis*-[Rh<sub>2</sub>(μ-O<sub>2</sub>CCH<sub>3</sub>)<sub>2</sub>(bpy)(dppz)]<sup>2+</sup> (**3**) was synthesized and its potential as a photodynamic therapy (PDT) agent was investigated. Although 27% hypochromicity of the absorption of **3** in the near-UV and visible regions is observed in the presence of duplex DNA, relative viscosity measurements reveal that the complex does not intercalate between the DNA bases. The DNA photocleavage with visible light by **3** proceeds via both oxygen dependent and independent mechanisms, and it is more efficient than that of related complexes. The increase in the cytotoxicity of **3** towards human skin cells is similar to that of hematoporphyrin, a key ingredient in a PDT drug currently in use. This feature makes this complex a useful candidate for further PDT studies.

Photodynamic therapy (PDT) provides a means to localize the action of drugs to tumor tissue, thus reducing the toxicity of the agent towards healthy cells.<sup>1,2</sup> Hematoporphyrin is a key component of Photofrin, a drug currently used in the photodynamic treatment of lung and esophageal cancers.<sup>1,2</sup> Although PDT has been successful, its requirement of O<sub>2</sub> to function represents a drawback, since many malignant and most aggressive cancer cells are hypoxic.<sup>1–3</sup> To circumvent this problem, new metal complexes have been recently investigated as potential oxygen-independent PDT agents.<sup>4–7</sup>

The oxygen-independent DNA photocleavage by *cis*-[Rh<sub>2</sub>(μ-O<sub>2</sub>CCH<sub>3</sub>)<sub>2</sub>(dppz)(η<sup>1</sup>-O<sub>2</sub>CCH<sub>3</sub>)(CH<sub>3</sub>OH)]<sup>+</sup> (**1**) and *cis*-[Rh<sub>2</sub>(μ-O<sub>2</sub>CCH<sub>3</sub>)<sub>2</sub>(dppz)<sub>2</sub>]<sup>2+</sup> (**2**) (dppz = dipyrido[3,2-*a*:2',3'-

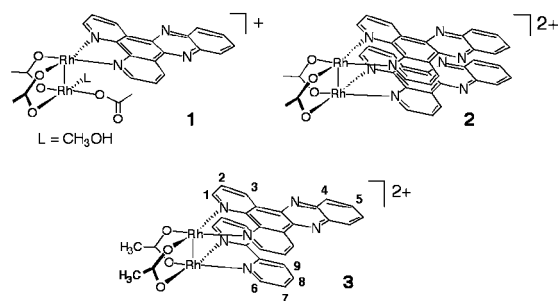


Figure 1. Schematic representation of the structures of 1–3.

*c*]phenazine) with visible light was recently reported (structures shown in Figure 1a).<sup>7</sup> The cytotoxicity of the DNA intercalating complex **1** towards Hs-27 human skin cells in the dark and upon irradiation with visible light is similar, with LC<sub>50</sub> values (concentration that results in 50% cell death) of 27 ± 2 and 21 ± 3 μM, respectively.<sup>7b</sup> In contrast, an increase in toxicity from LC<sub>50</sub> = 135 ± 8 μM in the dark to LC<sub>50</sub> = 39 ± 1 μM upon irradiation was observed for the nonintercalating complex **2**.<sup>7b</sup>

Although an increase in cytotoxicity upon irradiation was observed for **2**, a greater difference in LC<sub>50</sub> in the dark versus photolysis conditions is required for a compound to be useful as a PDT agent. To address this issue, a new dppz complex similar in structure to **2** was designed that is less hydrophobic and does not possess open equatorial coordination sites, features that result in rapid reactions with biological molecules and hence increased cytotoxicity of **1** in the dark. The new complex *cis*-[Rh<sub>2</sub>(μ-O<sub>2</sub>CCH<sub>3</sub>)<sub>2</sub>(dppz)(bpy)]<sup>2+</sup> (**3**) (bpy = 2,2'-bipyridine) was prepared (Figure 1a), which represents the first heteroleptic complex of this class. Complex **3** also incorporates a dppz ligand, which is believed to be a key feature in the photoreactivity of the system.<sup>7</sup> The present

\* To whom correspondence should be addressed. E-mail: turro.1@osu.edu (C.T.), dunbar@mail.chem.tamu.edu (K.R.D.).

<sup>†</sup> Texas A&M University.

<sup>‡</sup> The Ohio State University.

<sup>§</sup> Food and Drug Administration.

(1) DeRosa, M. C.; Crutchley, R. J. *Coord. Chem. Rev.* **2002**, 233–234, 351.

(2) Allen, C. M.; Sharman, W. M.; van Lier, J. E. *Tumor Targeting Cancer Ther.* **2002**, 329.

(3) Harris, A. L. *Nature Rev. Cancer* **2002**, 2, 38.

(4) Fu, P. K.-L.; Bradley, P. M.; van Loyen, D.; Dürr, H.; Bossmann, S. H. Turro, C. *Inorg. Chem.* **2002**, 41, 3808.

(5) (a) Swavey, S.; Brewer, K. J. *Inorg. Chem.* **2002**, 41, 6196. (b) Holder, A. A.; Swavey, S.; Brewer, K. J. *Inorg. Chem.* **2004**, 43, 303.

(6) Benites, P. J.; Holmberg, R. C.; Rawat, D. S.; Kraft, B. J.; Klein, L. J.; Peters, D. G.; Thorp, H. H.; Zaleski, J. M. *J. Am. Chem. Soc.* **2003**, 125, 6434.

(7) (a) Bradley, P. M.; Angeles-Boza, A. M.; Fu, P. K.-L.; Dunbar, K. R.; Turro, C. *Inorg. Chem.* **2004**, 43, 2450. (b) Angeles-Boza, A. M.; Bradley, P. M.; Fu, P. K.-L.; Wicke, S. E.; Bacsa, J.; Dunbar, K. R.; Turro, C. *Inorg. Chem.* **2004**, 43, 8510.

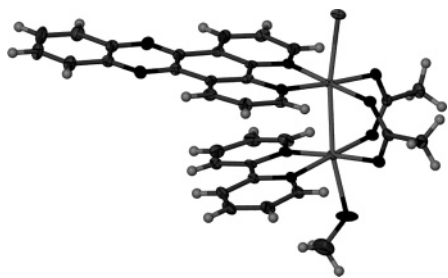


**Figure 2.** Crystal structure of **3** with ellipsoids at the 50% probability level.

report focuses on the DNA binding and photocleavage properties of **3**, along with its cytotoxicity and photocytotoxicity. The results are compared to those measured for hematoporphyrin, cisplatin, and related Rh<sub>2</sub>(II,II) complexes under similar experimental conditions.

The new heteroleptic complex **3** was prepared by refluxing *cis*-[Rh<sub>2</sub>(μ-O<sub>2</sub>CCH<sub>3</sub>)<sub>2</sub>(bpy)(η<sup>1</sup>-O<sub>2</sub>CCH<sub>3</sub>)(CH<sub>3</sub>OH)]-(O<sub>2</sub>CCH<sub>3</sub>)<sup>8</sup> (**4**; 0.64 mmol) with dppz (0.65 mmol) in CH<sub>3</sub>CN as described in the supporting information. In the aromatic region, the <sup>1</sup>H NMR (300 MHz) spectrum of **3** in CD<sub>3</sub>Cl exhibits peaks at δ/ppm (mult., int., assignment): 7.32 (d, 2H, 9), 7.45 (t, 2H, 7), 7.61 (t, 2H, 8), 7.92 (m, 2H, 2), 8.16 (m, 2H, 5), 8.47 (d, 2H, 6), 8.50 (m, 2H, 4), 8.78 (d, 2H, 1), 9.51 (d, 2H, 3), with the numbering scheme for the assignments shown in Figure 1. The <sup>1</sup>H NMR peak positions in the aromatic region of **3** are similar to those reported for related transition-metal complexes of dppz and bpy.<sup>7–9</sup> Greater shielding of the aromatic protons engaged in π-stacking interactions typically results in upfield shifts of the <sup>1</sup>H NMR resonances.<sup>10–12</sup> Such shifts were observed for **2** and *cis*-[Rh<sub>2</sub>(μ-O<sub>2</sub>CCH<sub>3</sub>)<sub>2</sub>(bpy)<sub>2</sub>]<sup>2+</sup> (**5**) relative to the corresponding monosubstituted compounds, **1** and **4**, respectively.<sup>7,8,13</sup> Owing to the greater extension of the dppz ligand as compared to bpy, the positions of the dppz resonances for the outermost ring protons, 4 and 5 in Figure 1, are not shifted relative to those in **1**. It should be noted that the upfield shifts for the bpy ligand protons in **3** are greater than those reported for **5** relative to **4**, indicative of greater shielding of the bpy ligand in **3** by dppz than by the other bpy ligand in **5**. Correspondingly, the shifts of the dppz protons 1–3 in **3** are not as large as those observed in **2** relative to **1**.

The structural features in solution are consistent with the crystal structure of the complex shown in Figure 2. Crystals suitable for X-ray crystallography were grown from a solution of **3** in CH<sub>3</sub>OH in the presence of NaBF<sub>4</sub> and NaCl that had been layered with diethyl ether. The molecular structure of the complex consists of a dinuclear Rh<sub>2</sub>(II,II)

core, with the chelating ligands, bpy and dppz, coordinated to one Rh atom each in a *syn* disposition and two acetate ligands bridging the metal centers. The axial positions of **3** are occupied by a chloride anion and a methanol molecule (Figure 2). The Rh–Rh distance in **3**, 2.5529(5) Å, is similar to those reported for *cis*-[Rh<sub>2</sub>(μ-O<sub>2</sub>CCH<sub>3</sub>)<sub>2</sub>(dppz)<sub>2</sub>]<sup>2+</sup> and *cis*-[Rh<sub>2</sub>(μ-O<sub>2</sub>CCH<sub>3</sub>)<sub>2</sub>(bpy)<sub>2</sub>]<sup>2+</sup>, 2.5519(6) and 2.548(4) Å, respectively.<sup>7b,8</sup> The internal twist angle across the metal–metal bond of 9.0(5)° in **3** is smaller than the one observed for the bis-dppz analogue (13°) but larger than that of the corresponding bis-bpy complex (6.2°).<sup>7b,8</sup>

The electronic absorption spectrum of **3** in ethanol is similar to those of the related complexes **2**, **4**, **5**, and *cis*-[Rh<sub>2</sub>(μ-O<sub>2</sub>CCH<sub>3</sub>)<sub>2</sub>(phen)<sub>2</sub>]<sup>2+</sup> (**6**; phen = 1,10-phenanthroline). The absorption at 432 nm (3100 M<sup>-1</sup> cm<sup>-1</sup>) in **3** is observed at 434 nm (5460 M<sup>-1</sup> cm<sup>-1</sup>) in **2** and at 432 nm (2080 M<sup>-1</sup> cm<sup>-1</sup>) in **5**.<sup>7b,13</sup> A ligand-centered (LC) ππ\* transition in **2** is observed at 363 nm (15 200 M<sup>-1</sup> cm<sup>-1</sup>), and two LC peaks appear in **5** at 280 nm (34 400 M<sup>-1</sup> cm<sup>-1</sup>) and 298 nm (27 500 M<sup>-1</sup> cm<sup>-1</sup>).<sup>7b,13</sup> As expected, **3** exhibits a broad absorption in the UV and near-UV, with ππ\* absorption peaks corresponding to bpy and dppz at 282 nm (61 000 M<sup>-1</sup> cm<sup>-1</sup>) and 366 nm (12 000 M<sup>-1</sup> cm<sup>-1</sup>), respectively. The lowest energy transition in **3** is weak (~350 M<sup>-1</sup> cm<sup>-1</sup>) and broad, appearing as a shoulder from ~460 to ~600 nm. Similar absorption features are observed at 590 nm (350 M<sup>-1</sup> cm<sup>-1</sup>), ~510 nm (~350 M<sup>-1</sup> cm<sup>-1</sup>), and 512 nm (380 M<sup>-1</sup> cm<sup>-1</sup>) for **1**, **2**, and **5**, respectively.<sup>7,13</sup> In the case of Rh<sub>2</sub>(μ-O<sub>2</sub>CCH<sub>3</sub>)<sub>4</sub>, the weak absorption at 585 nm (235 M<sup>-1</sup> cm<sup>-1</sup>) in water has been attributed to a RhRh(π\*) → RhRh(σ\*) transition.<sup>14,15</sup> No emission from complexes **1–3** was observed in CH<sub>3</sub>CN solutions at room temperature or as solids at 77 K. Similarly, Rh<sub>2</sub>(μ-O<sub>2</sub>CCH<sub>3</sub>)<sub>4</sub> is nonemissive, but its long-lived excited state (τ ~ 4–5 μs) can be monitored using transient absorption spectroscopy.<sup>16</sup> For complexes **1–3**, however, no transient absorption signal in the 300–700-nm region was observed in the nanosecond time scale in CH<sub>3</sub>CN (λ<sub>exc</sub> = 355 nm, fwhm ~ 8 ns, ~10 mJ/pulse).<sup>17</sup>

Titration of aqueous solutions containing 5 μM **3** (5 mM Tris, pH = 7.5, 50 mM NaCl) with calf-thymus DNA result in 27% hypochromicity at 366, 380, and 430 nm, however, no bathochromic shift is observed. No change in the relative viscosity of solutions containing 200 μM sonicated herring sperm DNA (5 mM Tris, pH = 7.5, 50 mM NaCl) is apparent in the presence of up to 60 μM **3**. Addition of 60 μM intercalator ethidium bromide results in the increase of the relative viscosity by a factor of 1.8 under similar experimental conditions. Because changes in the relative viscosity provide a reliable method for the assignment of DNA binding modes by intercalators,<sup>18</sup> the results above indicate that **3**

- (8) Crawford, C. A.; Matonic, J. H.; Streib, W. E.; Huffman, J. C.; Dunbar, K. R.; Christou, G. *Inorg. Chem.* **1993**, *32*, 3125.  
 (9) Liu, J.-G.; Ye, B.-H.; Zhang, Q.-L.; Zou, X.-H.; Zhen, Q.-X.; Tian, X.; Ji, L.-N. *J. Biol. Inorg. Chem.* **2000**, *5*, 119.  
 (10) Cubberley, M. S.; Iverson, B. L. *J. Am. Chem. Soc.* **2001**, *123*, 7560.  
 (11) Riesgo, E. C.; Hu, Y.-Z.; Bouvier, F.; Thummel, R. P. *Inorg. Chem.* **2001**, *40*, 3413.  
 (12) Yajima, T.; Maccarrone, G.; Takani, M.; Contino, A.; Arena, G.; Takamido, R.; Hanaki, M.; Funahashi, Y.; Odani, A.; Yamauchi, O. *Chem. Eur. J.* **2003**, *9*, 3341.  
 (13) Crawford, C. A.; Matonic, J. H.; Huffman, J. C.; Folting, K.; Dunbar, K. R.; Christou, G. *Inorg. Chem.* **1997**, *36*, 2361.

- (14) Boyar, E. B.; Robinson, S. D. *Coord. Chem. Rev.* **1983**, *50*, 109.  
 (15) Felthouse, T. R. *Prog. Inorg. Chem.* **1982**, *29*, 73.  
 (16) (a) Bradley, P. M.; Bursten, B. E.; Turro, C. *Inorg. Chem.* **2001**, *40*, 1376. (b) Bradley, P. M.; Fu, P. K.-L.; Turro, C. *Comments Inorg. Chem.* **2001**, *22*, 393.  
 (17) Instrumental details in: Warren, J. T.; Chen, W.; Johnston, D. H.; Turro, C. *Inorg. Chem.* **1999**, *38*, 6187.  
 (18) (a) Suh, D.; Oh, Y.-K.; Chaires, J. B. *Process Biochem.* **2001**, *37*, 521. (b) Haq, I.; Lincoln, P.; Suh, D.; Norden, B.; Chowdhry, B. Z.; Chaires, J. B. *J. Am. Chem. Soc.* **1995**, *117*, 4788.

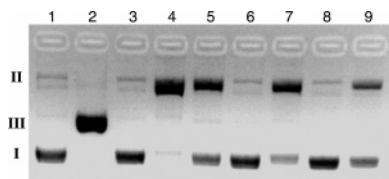


**Figure 3.** Ethidium bromide stained agarose gel (2%) of 100  $\mu\text{M}$  pUC18 plasmid showing the photocleavage ( $\lambda_{\text{irr}} > 395 \text{ nm}$ , 15 min) by a 10  $\mu\text{M}$  metal complex in 5 mM Tris and 50 mM NaCl at pH = 7.5. Lane 1: plasmid, dark. Lane 2: plasmid + *Sma*I. Lane 3: plasmid + **3**, dark. Lane 4: plasmid + **3**, irradiated, air. Lane 5: plasmid + **3**, irradiated, freeze-pump-thaw. Lane 6: plasmid + **1**, dark. Lane 7: plasmid + **1**, irradiated, air. Lane 8: plasmid + **2**, dark. Lane 9: plasmid + **2**, irradiated, air.

does not intercalate between the DNA bases. The hypochromic shift observed upon the addition of DNA likely arises from surface aggregation or  $\pi$ -stacking interactions of the cationic complex **3** aided by the DNA polyanion. The DNA binding constant of **3** was measured to be  $2.8 \times 10^3 \text{ M}^{-1}$  by equilibrium dialysis,<sup>19</sup> a value also inconsistent with intercalation of the complex. Similar results were recently reported for **2**.<sup>7b</sup>

The photocleavage of 100  $\mu\text{M}$  pUC18 supercoiled plasmid (form I) by 10  $\mu\text{M}$  **3** ( $\lambda_{\text{irr}} > 395 \text{ nm}$ , 15 min)<sup>20</sup> is shown in Figure 3. A comparison of the DNA-only control (lane 1) to that of **3** in the dark (lane 3) reveals that the complex does not cleave the plasmid without irradiation. The position on the gel of the linear (form III) plasmid linearized by *Sma*I is shown in lane 2 (Figure 3).<sup>21</sup> Nicked, circular plasmid (form II) is formed upon irradiation of **3** with visible light in air (lane 4) and in deoxygenated solutions (lane 5). Greater photocleavage is apparent for **3** (lane 4) compared to those of **1** (lane 7) and **2** (lane 9) in air. A comparison of the amount of photocleavage of **3** in air (lane 4) versus deoxygenated solutions (lane 5) reveals that, although greater cleavage is observed in the presence of oxygen, an oxygen-independent pathway to strand scission is also operative. It should be noted that related complexes that do not possess a dppz ligand, such as **5** and **6**, do not photocleave DNA.<sup>7</sup> Studies aimed at the elucidation of the mechanism and sequence selectivity of the DNA photocleavage by **1–3** are currently underway.

The cytotoxicity of **3** (30-min exposure) towards Hs-27 human skin fibroblasts,<sup>22</sup>  $\text{LC}_{50} = 208 \pm 10 \mu\text{M}$ , is 10-fold lower than that of hematoporphyrin in the dark ( $\text{LC}_{50} = 21 \pm 1 \mu\text{M}$ ). In addition, **3** is less cytotoxic than cisplatin under similar experimental conditions ( $\text{LC}_{50} = 131 \pm 10 \mu\text{M}$ ). Although **6** is the least cytotoxic complex,  $\text{LC}_{50} = 290 \pm 15 \mu\text{M}$ , no increase in its toxicity is observed upon exposure to visible light. Irradiation of Hs-27 cells exposed to **3** with visible light resulted in a  $79 \pm 10\%$  increase in cytotoxicity, with  $\text{LC}_{50} = 44 \pm 2 \mu\text{M}$ .<sup>23</sup> This increase is similar to that

observed for the key component of Photofrin, hematoporphyrin, which exhibits a  $82 \pm 10\%$  increase with  $\text{LC}_{50} = 3.8 \pm 0.2 \mu\text{M}$  under these irradiation conditions.

Single-cell electrophoresis experiments (Comet assays) were performed in the presence of 120  $\mu\text{M}$  **3** in the dark and under irradiation conditions with visible light in order to investigate if photolysis results in DNA damage.<sup>24–26</sup> When the human skin cells are exposed to **3** for 1 h in the dark, the stained DNA remains within the cells (Supporting Information). In contrast, upon irradiation of cells exposed to 120  $\mu\text{M}$  **3** for 30 min prior to irradiation (30 min, 400–700 nm, 5 J/cm<sup>2</sup>), approximately half of the cells exhibit a “comet tail” indicative of the migration of damaged DNA out of the cells under electrophoresis (Supporting Information). It should be noted, however, that the appearance of the “comet tail” in these assays can be due to direct DNA photocleavage by the complex or to apoptosis triggered by some other mechanism.<sup>27–29</sup> Experiments with bovine serum albumin (BSA) show that, although there are spectroscopic changes upon the addition of protein to **3**, the complex does not photocleave BSA upon irradiation with ultraviolet light (310 and 365 nm).<sup>30</sup>

Although the mechanism that results in cell death by photolysis of **3** remains unknown, the similarity in the increase in its cytotoxicity upon irradiation to that of hematoporphyrin is a promising indication that this complex is a useful candidate for further PDT studies. In particular, the lower dark cytotoxicity of **3** compared to that of hematoporphyrin is an advantageous feature for a PDT agent.

**Acknowledgment.** C.T. thanks the National Institutes of Health (Grant RO1 GM64040-01) for their generous support. K.R.D. thanks the State of Texas for an ARP grant (010366-0277-1999) and the Welch Foundation (A1449) for financial support, as well as Johnson-Matthey for a generous gift of  $\text{Rh}_2(\mu\text{-O}_2\text{CCH}_3)_4$ . The authors thank Prof. C. V. Kumar for protein photocleavage studies.

**Supporting Information Available:** X-ray crystallographic parameters, selected bond lengths and angles, the file in CIF format for the structure determination of **3**, synthesis, characterization, and <sup>1</sup>H NMR of **3**, and single-cell electrophoresis data and methods. This material is available free of charge via the Internet at <http://pubs.acs.org>.

IC0500715

(19) Equilibrium dialysis was conducted with purified calf-thymus DNA (Sigma) using >100 000 Da dialysis membranes (Sigma) against 10 mM Tris (pH = 7.5) and 20 mM NaCl for 48 h.

(20) The irradiation source was a 150-W Xe arc lamp (PTI).

(21) Plasmid linearized using 10 units of *Sma*I (Invitrogen) at 37 °C for 1 h.

(22) Human skin fibroblasts (Hs-27) were obtained from the American Type Culture Collection, cell line CRL-1634 (Manassas). The cytotoxicity was determined as described in detail in ref 7b.

(23) The source of visible radiation (400–700 nm) for the photocytotoxicity studies was a photoreactor (Luzchem, Ontario, Canada) composed of 12 8-W GE watt-miser bulbs (General Electric).

(24) Fairbairn, D. W.; Olive, P. L.; O’Neill, K. L. *Mutat. Res.* **1995**, 339, 37.

(25) Speit, G.; Hartmann, A. In *Methods Molecular Biology: DNA Repairs Protocols*; Henderson, D. S., Ed.; Humana Press: New York, 1999; Vol. 113, pp 203–212.

(26) Rojas, E.; Lopez, M. C.; Valverde, M. *J. Chromatogr., B: Biomed. Sci. Appl.* **1999**, 722, 225.

(27) Hartmann, A.; Agurell, E.; Beevers, C.; Brender-Schwaab, S.; Burlinson, B.; Clay, P.; Collins, A.; Smith, A.; Speit, G.; Thybaud, V.; Rice, R. R. *Mutagenesis* **2003**, 18, 45.

(28) Gómez-Lechón, M. J.; O’Connor, E.; Castell, J. V.; Jover, R. *Toxicol. Sci.* **2002**, 65, 299.

(29) Lash, L. H.; Hueni, S. E.; Putt, D. A. *Toxicol. Appl. Pharmacol.* **2001**, 177, 1.

(30) Kumar, C. V.; Thota, J. *Inorg. Chem.* **2005**, 44, 825.